

Extended Data Fig. 1: Metabolic response in ischaemic mouse and naked mole-rat heart and liver

a,b Heatmaps of all metabolites detected in **a**, heart and **b**, liver from mouse and naked mole-rats in 0, 5, 10, 30 and 60 min of ischaemia. Black box in **a**, outlines the cluster represented in Fig. 1e. **c-e**, Levels of **c**, maltotetraose **d**, maltotriose and **e**, disaccharide in liver from mouse and naked mole-rats (n=3 for mouse liver at 10 mins, n=4 each for other groups for **a-e**). Error bar represents mean \pm s.e.m. n numbers refer to individual animals. Two-way ANOVA with Tukey's test was used for correction of multiple comparisons in **c-e**. *p < 0.05, **p < 0.01, ***p < 0.001 within species comparison at different timepoints.

Extended Data Fig. 2: Expression of glycogen related genes in mouse and naked mole-rat liver

a, Heatmap of transcriptomic analysis between mouse and naked mole-rat heart and liver for the GO term glycogen metabolic process. **b,c**, Western blot analysis and quantification normalised to ponceau loading control of GP isoforms in mouse and naked mole-rat liver (n=4) **b**, muscle isoform PYGM and **c**, liver isoform PYGL (for gel source data see Supplementary Data 5). (n=4 each). Error bar represents mean \pm s.e.m. n numbers refer to individual animals, unless otherwise stated. Two-tailed, unpaired Student t-tests were used for statistical analysis in **b,c**.

Extended Data Fig. 3: Glycolytic intermediates in ischaemic heart of mouse and naked mole-rat

Levels of glycolytic intermediates **a**, 2/3-phosphoglycerate (2/3PGA) and **b**, phosphoenolpyruvate (PEP) in baseline and ischaemia in mouse and naked mole-rat hearts (n=4 each). Error bar represents mean \pm s.e.m. n numbers refer to individual animals. Two-way ANOVA with Tukey's test was used for correction of multiple comparisons. *p < 0.05, **p < 0.01, ***p < 0.001, within species comparison at different timepoints, #p < 0.05, ##p < 0.01, ###p < 0.001 between species comparison for corresponding timepoints.

Extended Data Fig 4: Co-option of Amy1 in naked mole-rat heart for efficient glycogen breakdown

a,b, Mapped reads for amylase from RNAseq analysis onto the **a**, mouse and **b**, naked mole-rat genomes. **a**, Mouse has 7 copies of amylase genes and **b**, naked mole-rat has 3 copies of amylase genes. Amylase reads from heart and liver map to Amy1 gene in both naked mole and mouse. Intensity of mapped reads is much higher in naked mole-rat for corresponding mouse tissue (n=3). **c**, in-gel proteomics analysis of selected size intervals cut from gel of proteins from mouse and naked mole-rat heart, liver and brain tissues separated by SDS-PAGE. Numbers indicate peak intensity (log2) of amylase protein found in corresponding gel piece with size indicated on the left, ND denotes that amylase was not detected (n=1).

Extended Data Fig. 5: Inhibition of amylase decreases glycolytic and TCA cycle intermediates in hypoxia

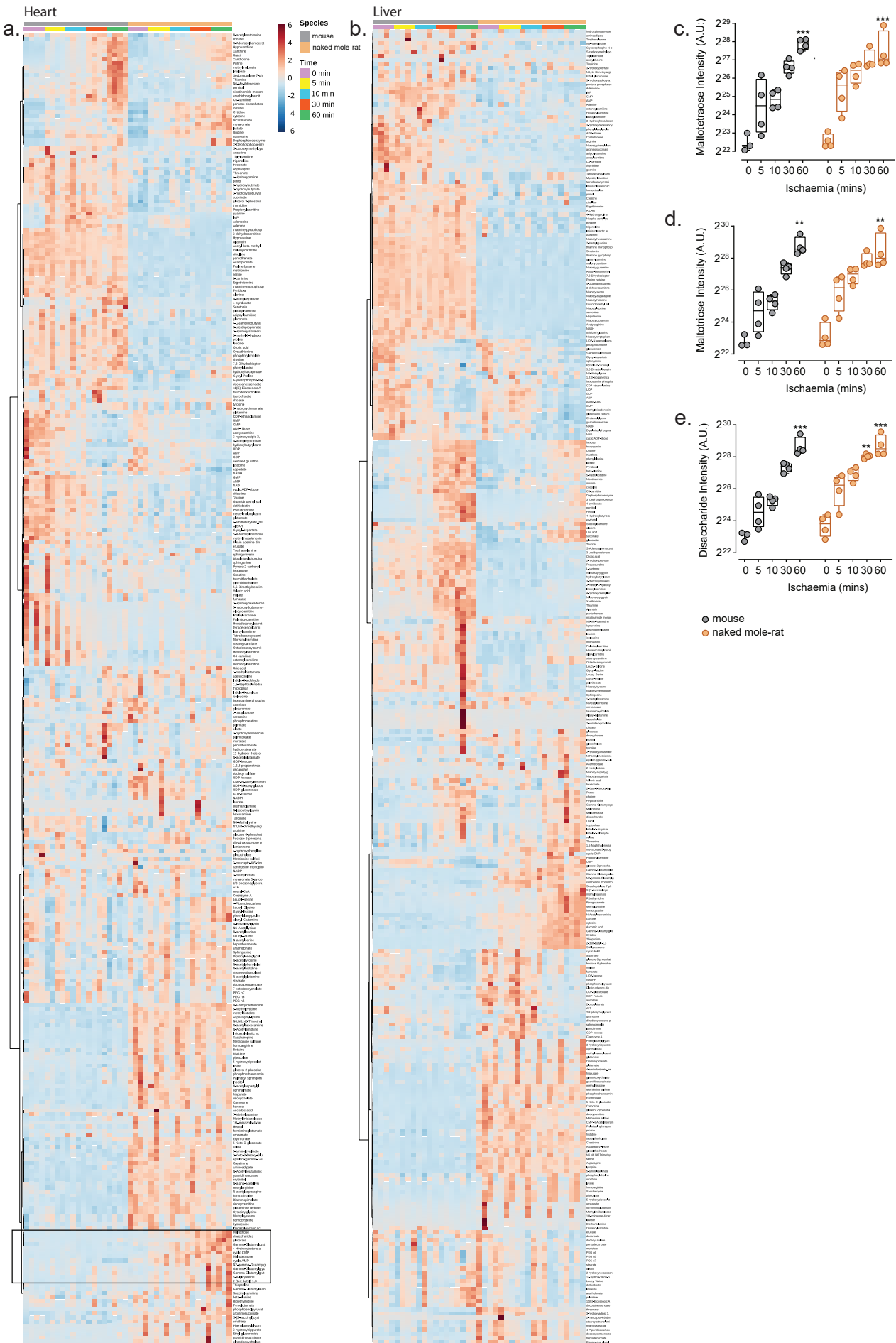
a, Summary of glycogen breakdown pathways in naked mole-rat and mouse heart, effect of acarbose on amylase in indicated. Metabolites that decrease with amylase inhibition in 0.1% hypoxia compared to hypoxia control are marked in blue, increased in yellow, unchanged metabolites in grey. Relative changes in levels normalized to 30 min hypoxia in naked mole-rat and mouse heart of **b,c** the polysaccharides **b**, maltotriose, and **c**, maltose **d**, glucose, **e**, glucose-1-phosphate (G1P). Intermediates of upper glycolysis **f**, Glucose-6-phosphate, **g**, fructose-6-phosphate. Intermediates of lower glycolysis **h**, fructose-1,6-bisphosphate (F1,6BP) **i**, 1,3-bisphosphoglycerate (1,3BPG) **j**, 3-phosphoglycerate (3PGA), **k**, pyruvate **l**, lactate. TCA cycle intermediates **m**, citrate **n**, isocitrate **o**, acetic acid **p**, alpha-ketoglutarate (aKG) **q**, succinate **r**, fumarate **s**, malate **t**, succinate/fumarate ratio. Intermediates of the polyol pathway **u**, sorbitol and **v**, fructose and intermediate of fructose metabolism **w**, fructose-1-phosphate (F1P) (n=4 for mouse, n=3 for naked mole-rat). Error

bar represents mean \pm s.e.m. n numbers refer to individual animals. Two-tailed, unpaired Student t-tests were used for statistical analysis in b-w. *p < 0.05, **p < 0.01, ***p < 0.001.

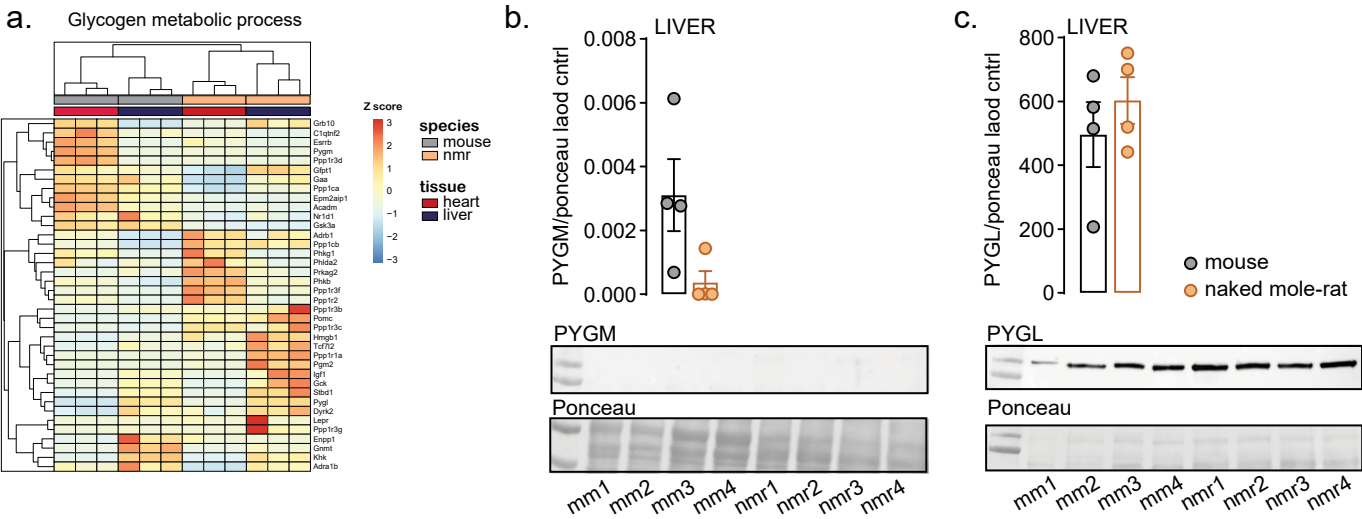
Extended Data Fig. 6: Non-canonical glycogen pathways are altered in naked mole-rat heart

a, expression of MGAM in heart determined by RNAseq (n=3), **b**, Fluorescence intensity quantification of GAA immunostaining of heart tissue sections in mouse and naked mole-rat at baseline and 30 mins ischaemia **c**, Mander's coefficient representing colocalization of GAA with glycogen in heart sections of mouse and naked mole-rat at baseline and 30 mins ischaemia (19-23 individual images were analysed, n=3-4). **m**, Representative images for **b** and **c**. Error bar represents mean \pm s.e.m. n numbers refer to individual animals. Two-way ANOVA with Tukey's test was used for correction of multiple comparisons in **b,c**, *p < 0.05, **p < 0.01, ***p < 0.001.

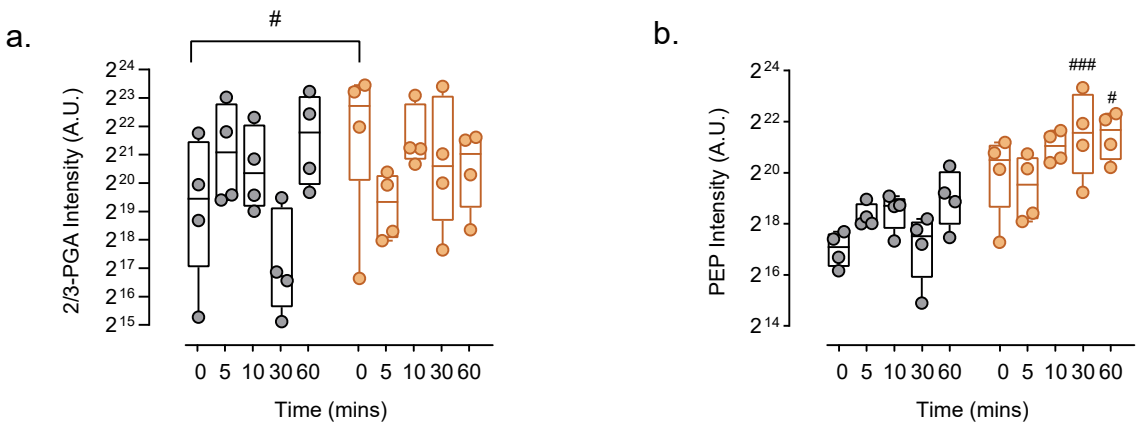
Extended Data Fig.1: Metabolic response in ischaemic mouse and naked mole-rat heart and liver



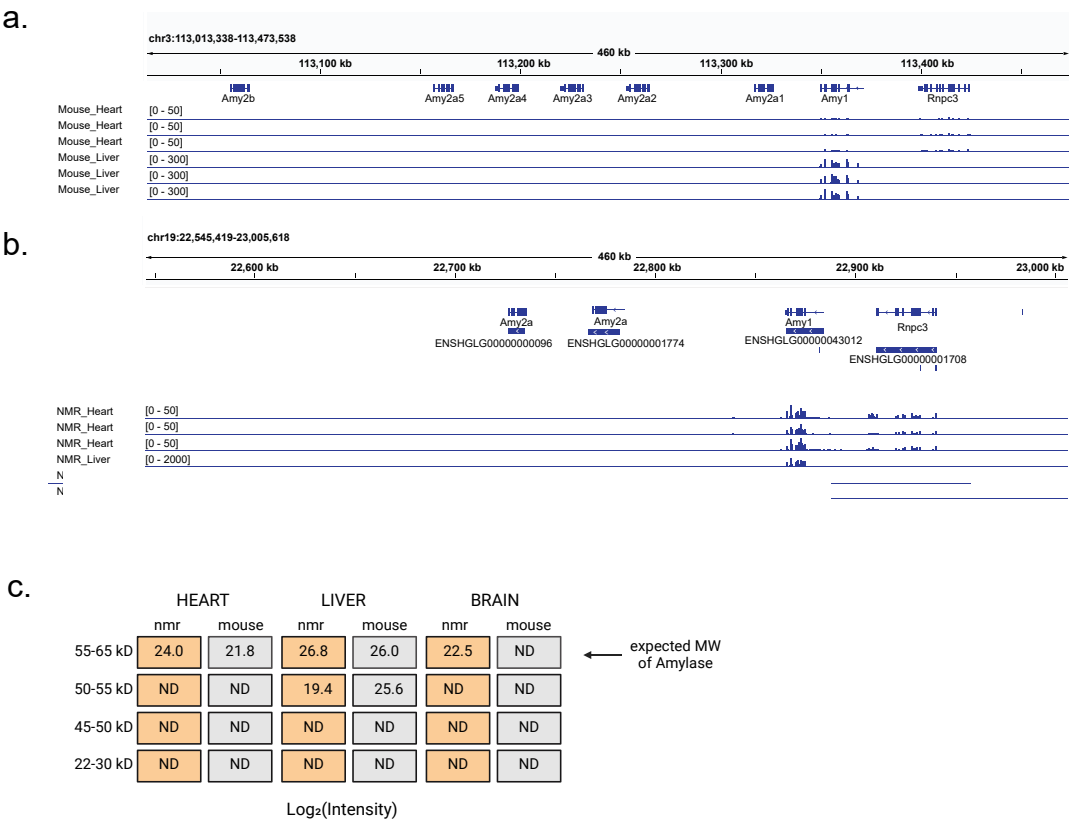
Extended Data Fig 2: Expression of glycogen related genes in mouse and naked mole-rat liver



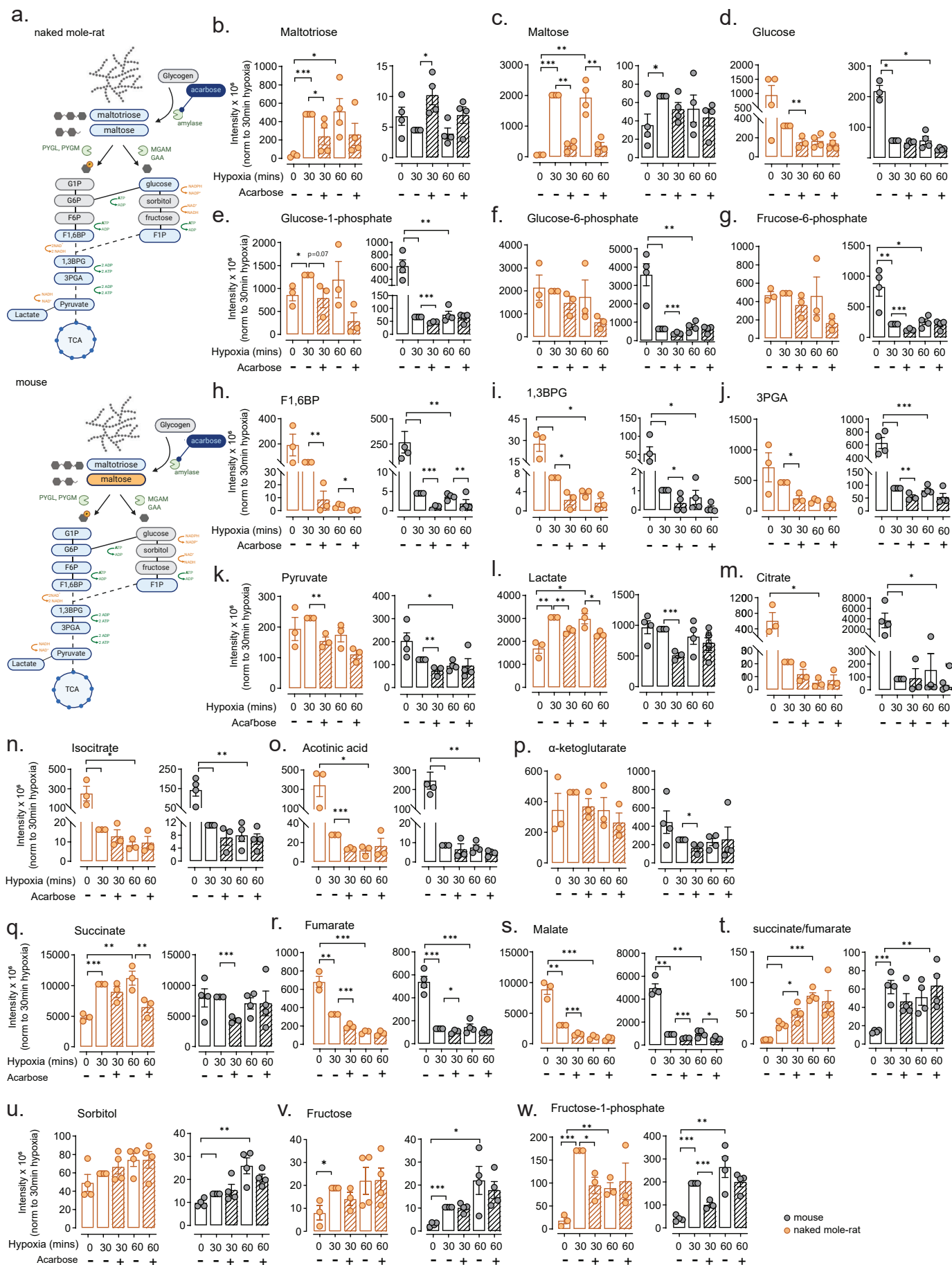
Extended Data Fig. 3: Glycolytic intermediates in ischaemic heart of mouse and naked mole-rat



Extended Data Fig.4: Co-option of Amy1 in naked mole-rat heart for efficient glycogen breakdown



Extended Data Fig.5: Inhibition of amylase decreases glycolytic intermediates in hypoxia



Extended data Fig.6: Non-canonical glycogen pathways are altered in naked mole-rat heart

